

Analysis of a functionally graded nanocomposite sandwich beam considering porosity distribution on variable elastic foundation using DQM: Buckling and vibration behaviors

Mohammad Mehdi Nejadi and Mehdi Mohammadimehr*

Department of Solid Mechanics, Faculty of Mechanical Engineering, University of Kashan, Kashan, Iran

(Received December 2, 2019, Revised February 24, 2020, Accepted February 29, 2020)

Abstract. In the present study, according to the important of porosity in low specific weight in comparison of high stiffness of carbon nanotubes reinforced composite, buckling and free vibration analysis of sandwich composite beam in two configurations, of laminates using differential quadrature method (DQM) is studied. Also, the effects of porosity coefficient and three types of porosity distribution on critical buckling load and natural frequency are discussed. It is shown the buckling loads and natural frequencies of laminate 1 are significantly larger than the results of laminate 2. When configuration 2 (the core is made of FRC) and laminate 1 ([0/90/0/45/90]_s) are used, the first natural frequency rises noticeably. It is also demonstrated that the influence of the core height in the case of lower carbon volume fractions is negligible. Even though, when volume fraction of fiber increases, the critical buckling load enhances smoothly. It should be noticed the amount of decline has inverse relationship with the beam aspect ratio. Investigating three porosity patterns, beam with the distribution of porosity Type 2 has the maximum critical buckling load and first natural frequency. Among three elastic foundations (constant, linear and parabolic), buckling load and natural frequency in linear variation has the least amount. For all kind of elastic foundations, when the porosity coefficient increases, critical buckling load and natural frequency decline significantly.

Keywords: buckling and vibration analysis; DQM; variable-elastic foundation; nano sandwich composite beam; various porosity distributions

1. Introduction

Porous materials are widely used in structural design of wide number of fields and industries including transportation, aerospace, energy and construction due to their low specific weight, and increased machinability. Carbon Nano Tube (CNT) has been accepted as an excellent material for the reinforcement of polymer composites due to their high elastic modulus and low density (Esawi and Farag 2007). CNTs are also recently combined with porous materials to be used in various areas specially composites (Gui *et al.* 2011). Porous materials with functional properties have some similarities with the functionally graded materials. The porosity can cause a smooth or rough change in mechanical properties depending upon some parameters such as porosity distributions and volume fraction of composite.

During the last several years, the problem of buckling of the porous materials with varying properties has been discussed by many authors. Thermal buckling behavior of functionally graded Carbon Nano Tube -Reinforced Composite (CNTRC) plates was investigated by Shen and Zhang (2010). The buckling analysis of thin functionally graded rectangular plates based on the classical or first order shear deformation theory under various loads were

discussed by Mohammadi *et al.* (2010). Jabbari *et al.* (2013, 2014) examined porosity distribution influence on buckling characteristics of plates. Buckling of metal foam porous beams using a shear deformation beam model was studied by Chen *et al.* (2015). Elastic properties were evaluated for different volume fractions along the material principal directions using finite element method by Sudheer *et al.* (2015). The design of laminates with a minimum number of layers for obtaining the given elastic properties was addressed by Montemurro *et al.* (2015). Also, the porosity effects were also investigated in recent works such as Medani *et al.* (2019), Berghouti *et al.* (2019), Bourada *et al.* (2019), Batou *et al.* (2019), Yazdani and Mohammadimehr (2019). Babaeeian and Mohammadimehr (2020) considered the time elapsed effect on residual stress measurement in a composite plate by DIC method.

Some of useful recent references about nano composites structures are Ghorbanpour Arani *et al.* (2012), Mohammadimehr *et al.* (2017a, 2018), Medani *et al.* (2019), Draoui *et al.* (2019), Alimirzaei *et al.* (2019), Karami *et al.* (2019), Bamdad *et al.* (2019). Also, the influences of surface stress on the nanocomposite are studied by Mohammadimehr and Alimirzaei (2016), Ghorbanpour Arani *et al.* (2016), Mohammadimehr *et al.* (2017b). Many works have considered the effect of elastic foundations such as Addou *et al.* (2019), Chaabane *et al.* (2019), Boulefrakh *et al.* (2019). Moreover, Boukhlif *et al.* (2019) investigated FG thick plate in this category. Semmah *et al.* (2019) studied thermal buckling and Karami *et al.*

*Corresponding author, Ph.D.
E-mail: mmohammadimehr@kashanu.ac.ir

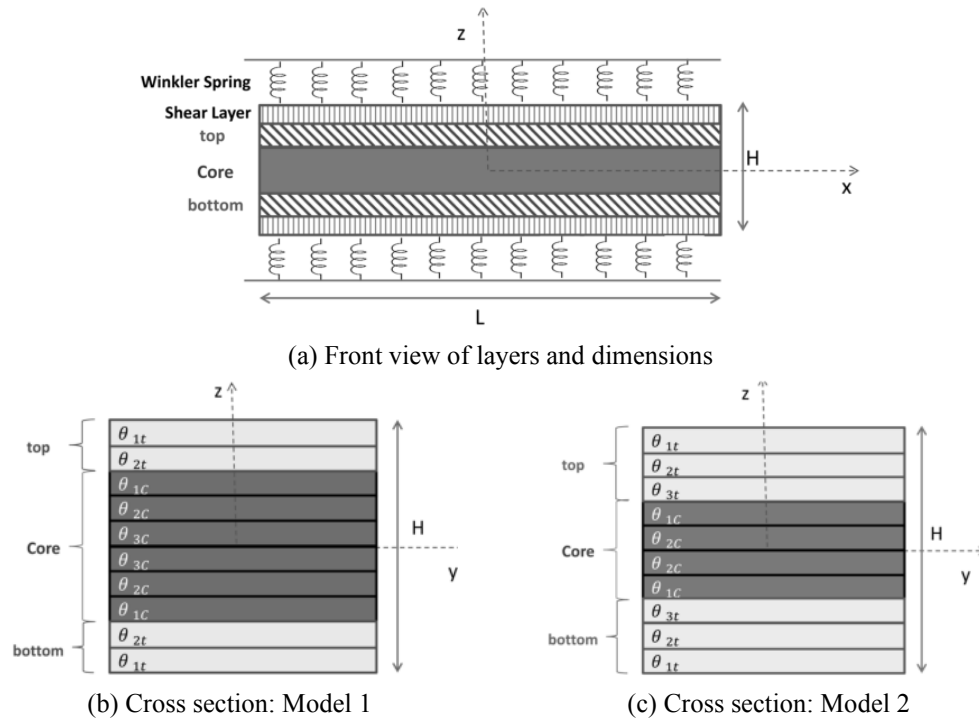


Fig. 1 Sandwich composite beam resting on elastic foundations

(2019), Zaoui *et al.* (2019) presented new quasi-3D shear deformation theories for free vibration of functionally graded plates.

The high order buckling of two types of sandwich beams including AL-foam or PVC-foam flexible core and CNTs reinforced nanocomposite face sheets were investigated by Mohammadimehr and Shahedi (2017). Also, in the other work, Shahedi and Mohammadimehr (2020) considered nonlinear high-order dynamic stability of AL-foam flexible cored sandwich beam with variable mechanical properties and carbon nanotubes-reinforced composite face sheets in thermal environment. A finite element method was proposed by Zghal *et al.* (2017) for linear static analysis of functionally graded Carbon Nano Tube -Reinforced Composite (CNTRC). The results are illustrated by three numerical examples in order to outline the performance. Postbuckling analysis of nonhomogeneous nano plates considering even and uneven distributions of porosity with the usage of nonpolynomial shear deformation theory was demonstrated by Barati and Zenkour (2018). Rajabi and Mohammadimehr (2019a) presented hydro-thermo-mechanical biaxial buckling analysis of sandwich micro-plate with isotropic/orthotropic cores and piezoelectric/polymeric nanocomposite face sheets based on FSDT. The buckling of simply supported laminated composite plates is studied by Xiang *et al.* (2015) using various higher-order shear deformation theories. The nonlocal critical buckling loads in relation to buckling mode number, and aspect ratio, in the presence and absence of an elastic medium, were examined by Chemi *et al.* (2018). Al-Kamal (2019) presented nominal axial and flexural strengths of high-strength concrete columns. Yazdani *et al.* (2019) presented vibration analysis of double-bonded micro sandwich cylindrical shells under multi-physical loadings.

Parate and Kumar (2019) considered shear strength model for reinforced concrete beam-column joints based on hybrid approach. Wu *et al.* (2019) experimentally studied on shear damage and lateral stiffness of transfer column in SRC-RC hybrid structure. Rajabi and Mohammadimehr (2019b) depicted bending analysis of a micro sandwich skew plate using extended Kantorovich method based on Eshelby-Mori-Tanaka approach. Anvari *et al.* (2020) illustrated vibration behavior of a micro cylindrical sandwich panel reinforced by graphene platelet.

Numerical methods are widely used to give approximately accurate solutions for complicated problems. For instance, a detailed analysis of natural frequencies of laminated composite plates using the mesh free moving Kriging interpolation method was presented by Bui *et al.* (2011). The nonlinear vibration frequencies of functionally graded CNTRC were numerically investigated using finite element method by Kulmani Mehar *et al.* (2017). A novel and effective computational approach within the context of isogeometric analysis was developed for analyzing size-dependent mechanical behaviors of functionally graded microbeams by Yu *et al.* (2019). Mechanical behavior of porous beams by an effective computational approach based on isogeometric analysis (IGA) was analyzed (Fang *et al.* 2019). The quasi-3D theory is employed to take into account normal and shear deformations. Liu *et al.* (2019) presented an effective plate formulation based on isogeometric analysis (IGA) and non-classical Kirchhoff plate theory for the study of static bending and buckling behaviors of nanoplates. Yu *et al.* (2019) developed a two-directional functionally graded microbeam model for natural frequency and mechanical bending analysis by using NURBS-based isogeometric analysis combined with a non-classical quasi-3D beam theory.

In the present paper, according to the importance of porosity to reduce specific weight of composites, the buckling and free vibration analysis of sandwich composite beam consists of Carbon Nano Tube Reinforced Composite (CNTRC) and Fiber Reinforced Composite (FRC) beam will be analyzed. For this purpose, the problem was investigated in two different configurations to discuss the sandwiches materials. Plus three various laminates were utilized to investigate the angles and two models to study the core height. They all are solved by differential quadrature method (DQM). Moreover, influences of porosity coefficient and porosity distribution types on critical buckling load and natural frequency will be discussed. In addition, the effect of variation of elastic foundation as forces against buckling along the beam length will be studied. At the end, the first three modes of buckling and vibration for different spring constants will be demonstrated. Also, the most important advantage of the present work is designing a nanocomposite sandwich beam consists of a four-layer ([45/90]_s) FRC core and a three-layer ([0/90/0]) CNTRC at top and bottom by considering symmetric porosity distribution (the most porosity in the middle), on elastic foundation, which is more resistant against buckling and vibration.

2. Problem statement

The sandwich composite beam composed of a core and two layers in the top and bottom is resting on shear layer and Winkler spring with two different configurations (Fig. 1(a)).

In Configuration 1, the core is made of Carbon Nano Tube -Reinforced Composite (CNTRC) and the top and bottom layers are made of Fiber Reinforced Composite (FRC). In Configuration 2, the material of core is replaced with the material of top and bottom layers and the other way around.

In addition, two different models are investigated. In Model 1, the height of each peripheral layer is one-third of core height (Fig. 1(b)). Even though, in Model 2, the height of top or bottom layer is three-fourth of core height (Fig. 1(c)). All results in the present paper are obtained with Model 1 if it is not mentioned otherwise. For discussing the influence of angles on the buckling load, three laminates are defined in Table 1.

Governing equation for the buckling and free vibration of Euler-Bernoulli composite beam are defined in Eq. (1) (Mohammadimehr and Shahedi 2017) and Eq. (2) respectively (Montemurro *et al.* 2012). Substituting Eq. (3) into the governing equation for vibration, Eq. (4) is formed.

$$\frac{d^4 w}{dx^4} - \lambda_1 \frac{d^2 w}{dx^2} + \eta w - \mu v^2 w = 0 \tag{1}$$

$$\frac{\partial^4 w(x, t)}{\partial x^4} + \frac{\rho A}{E_{ef} I} \frac{\partial^2 w(x, t)}{\partial t^2} + \frac{K_f(x)}{E_{ef} I} w(x, t) = 0 \tag{2}$$

$$w(x, t) = \bar{w}(x) e^{i\omega t} \tag{3}$$

$$\frac{\partial^4 \bar{w}(x)}{\partial x^4} + \left(\frac{K_f(x) - \rho A \omega^2}{E_{ef} I} \right) \bar{w}(x) = 0 \tag{4}$$

where $\eta = \frac{K_f(x)l^4}{E_{ef} I}$ represents the stiffness parameter of Winkler foundation and μ is shear modulus of Pasternak foundation. P_{cr} is critical buckling load, I is moment of inertia for the cross section, A is cross section area, ρ is density, ω is circular natural frequency, $K_f(x)$ is spring constant which could be constant or vary linearly or parabolically through the length of the beam and α is fixed coefficient is as follows

$$K_f(x) = K_{f0} \tag{5-1}$$

$$K_f(x) = K_{f0}(1 - \alpha x) \tag{5-2}$$

$$K_f(x) = K_{f0}(1 - \alpha x^2) \tag{5-3}$$

E_{ef} is effective modulus of elasticity which can be presented by the Eq. (6).

$$E_{ef} = \frac{8}{h^3} \sum_{j=1}^m (E_x)_j (z_j^3 - z_{j-1}^3) \tag{6}$$

where m is the number of layers, h is the height of the beam, z is distance between the outer plane of j^{th} layer and the neutral axis.

Dimensionless critical buckling load can be obtained by Eq. (7).

$$N_{cr} = \frac{P_{cr}}{A_{110}} \tag{7}$$

Where A_{11} expressed by Eq. (8) is extensional stiffness of beam and A_{110} represents A_{11} for the beam made of pure matrix.

$$A_{11} = \sum_{k=1}^n \int_{h_{k-1}}^{h_k} (\overline{Q_{11}})_k dz \tag{8}$$

In the mentioned equation, h_k and h_{k-1} are the z values for the top and bottom and $\overline{Q_{11}}$ is the transformed elastic constant of the k^{th} layer could be calculated by Eq. (9).

$$\overline{Q_{11}} = Q_{11}c^4 + Q_{11}s^4 + (2Q_{12} + 4Q_{33})s^2c^2 \tag{9}$$

Where

$$\begin{aligned} s &= \sin\theta & c &= \cos\theta \\ Q_{11} &= \frac{E_1}{1 - \nu_{12}\nu_{21}} & Q_{22} &= \frac{E_2}{1 - \nu_{12}\nu_{21}} \\ Q_{12} &= \frac{\nu_{12}E_2}{1 - \nu_{12}\nu_{21}} & Q_{33} &= G_{12} \end{aligned}$$

Table 1 The angles of sandwich nanocomposite beam for Laminate 1 and 2

Laminate	θ_{1t}	θ_{2t}	θ_{1c}	θ_{2c}	θ_{3c}
1	0	90	0	45	90
2	45	-45	45	-45	45

3. Solving method

Table 2 The mechanical properties of CNTRC based on extended rule of mixture

V_{cnt}	η_1	η_2	η_3	E_{11}	E_{22}	G_{12}	ν_{12}
0.12	1.2833	1.0556	1.0556	2.3626	2.9000	1.1110	3.2218
0.17	1.3414	1.7101	1.7101	2.3157	4.9000	1.9012	5.4437
0.28	1.3238	1.7380	1.7380	2.1913	5.5000	2.2056	6.1103

To solve the Eq. (1) by Differential Quadrature Method (DQM), the first-order, the second-order, the third-order and the fourth derivatives of any arbitrary function in arbitrary point can be approximated in all intervals as follows in Eq. (10)

$$\frac{d^r f}{dx^r}(x = x_i) = \sum_{k=1}^n A_{ik}^r f(x_k) \tag{10}$$

where A^r is weighted coefficient matrices which are defined by Eqs. (11), (12) and (13).

$$A_{ij}^{(1)} = \frac{\prod_{m=1, m \neq i}^N (x_i - x_m)}{\prod_{m=1, m \neq j}^N (x_i - x_m)} \quad (i, j = 1, 2, 3, \dots, N; i \neq j) \tag{11}$$

$$A_{ij}^{(1)} = \sum_{m=1}^N \frac{1}{m \neq j} \frac{1}{(x_i - x_m)} \quad (i, j = 1, 2, 3, \dots, N) \tag{12}$$

$$A^r = A^{(r-1)} A^r \quad 2 \leq r \leq N - 1 \tag{13}$$

Chebyshev points which are well-recognized set of the grid points for interval $[0, L]$ are presented by Eq. (14).

$$x_i = \frac{1}{2} \left\{ 1 - \cos \left[\frac{(i-1)\pi}{(N-1)} \right] \right\} \tag{14}$$

4. Material properties

Mechanical properties of nanocomposite beam made of CNT reinforced polymer can be estimated using extended rule of mixture as follows in Eqs. (11) to (14) (Gui *et al.* 2011)

$$E_{11} = \eta_1 V_{CNT} E_{11}^{CNT} + V_m E^m \tag{15}$$

$$\frac{\eta_2}{E_{22}} = \frac{V_{CNT}}{E_{22}^{CNT}} + \frac{V_m}{E^m} \tag{16}$$

$$\frac{\eta_3}{G_{12}} = \frac{V_{CNT}}{G_{12}^{CNT}} + \frac{V_m}{G^m} \tag{17}$$

$$\nu_{12} = V_{CNT} \nu_{12}^{CNT} + V_m \nu^m \tag{18}$$

Where E_{11}^{CNT} and E_{22}^{CNT} represent the Young's modulus of the Single-Walled Carbon Nano Tube parallel and perpendicular to the beam and considered to be 600 and 10 GPa, respectively. G_{12}^{CNT} and ν_{12}^{CNT} which are the shear modulus and Poisson ratio of CNT be equal to 17.2 GPa and 0.19. Also $E^m = 2.5$ GPa and $G^m = 0.933$ GPa and $\nu^m = 0.34$ indicate the corresponding properties for the PMMA matrix. Efficiency factors are denoted by η_1, η_2 and η_3 which are related to the nano-scale size effect. The mentioned properties of composite are calculated in Table 2.

The mechanical properties of composite made of carbon

fiber reinforced polymer (FRP) could be obtained by rule of mixture expressed its efficiency factors equal 1. Instead of CNT's properties, fiber's ones will be used.

Elastic properties of carbon fiber are represented as follows: $E_{11}^f = 600$ GPa, $E_{22}^f = 14$ GPa, $G_{12}^f = 9$ GPa, $\nu_{12}^f = 0.2$ and volume fractions of fibers are considered to be 0.4.

For adding porosity consideration, the elastic properties of matrix of composite are assumed to vary by two types of porosity distribution across the height.

Three types of porosity distributions are presented by Eqs. (19) to (21) as follows

$$\text{Type1: } E(z) = E_0 \left[1 - e_1 \left(\cos \left(\frac{\pi}{h} z \right) \right) \right] \tag{19}$$

$$\text{Type2: } E(z) = E_0 \left[1 - e_1 \left(1 - \cos \left(\frac{\pi}{h} z \right) \right) \right] \tag{20}$$

$$\text{Type3: } E(z) = E_0 \left[1 - e_1 \left(1 - \left(\frac{z}{h} + \frac{1}{2} \right) \right) \right] \tag{21}$$

where E_1 and E_0 are the Young's modulus of elasticity. It should be mentioned that the same pattern is considered for shear modulus, Poisson's ratio and density. Coefficient of beam porosity represented by e_1 is obtained by Eq. (22).

According to Eq. (22), in case porosity coefficient 0, there is no porosity and the bottom and top of the layer have the same Young's modulus; while when the porosity coefficient is equal to 1, the maximum porosity occurs between two layers.

$$e_1 = 1 - \frac{E_1}{E_0} \tag{22}$$

5.1 Results and discussion of buckling

Dimensionless critical buckling load of CNTRC with and without elastic foundations is presented in Table 3. It should be mentioned η and μ represent Winkler and shear spring constants, respectively. The buckling loads are compared with the results of Yas and Samadi (2012) for three volume fraction of CNT and two different boundary conditions (Clamped-Free and Hinged-Hinged). As can be seen, the results are in good agreements.

Table 3 Comparing the critical buckling loads of CNTRC with the results of Yas and Samadi (2012) for aspect ratio 15

(η, μ)	Boundary Conditions	V_{cnt}	\bar{N}_{cr} Present Work	\bar{N}_{cr} Yas and Samadi (2012)	Difference (%)
(0,0)	CF	0.12	0.03147	0.031234	0.74
	CF	0.17	0.04620	0.046318	-0.25
	CF	0.28	0.07458	0.072178	3.32
(0.1,0.02)	CF	0.12	0.04237029	0.041901	1.12
	CF	0.17	0.05883876	0.057736	1.91
	CF	0.28	0.08628671	0.083912	2.83
(0.1,0)	CF	0.12	0.04793184	0.047542	0.82
	CF	0.17	0.06253564	0.063385	-1.34
	CF	0.28	0.09218102	0.089557	2.93

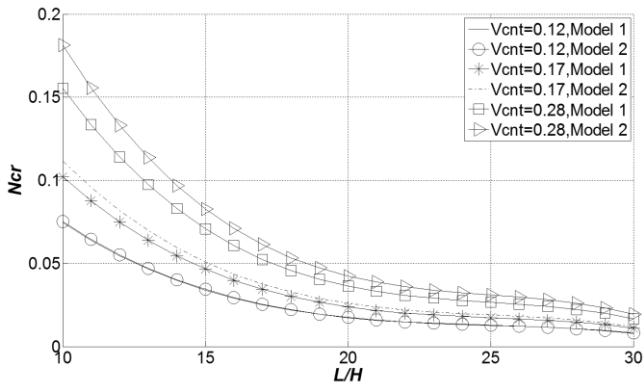


Fig. 2 critical buckling load against aspect ratio for two models

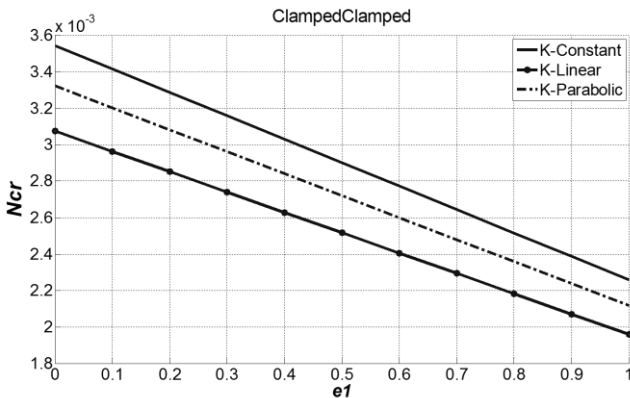


Fig. 3 critical buckling load against porosity coefficient for three kind of elastic foundations

Fig. 2 shows two models described earlier to study the effect of the core height. It can be seen that in the case of lower carbon volume fractions, the influence is negligible. Even though, when volume fraction of fiber rises, differences increase gently. In addition, the effect is even more in the smaller beam aspect ratios.

Fig. 3 demonstrates critical buckling load against porosity coefficient in three different elastic foundations with $K_f=1000$ and $\alpha=0.2$. Clamped boundary condition is applied at two ends of the beam. It can be seen, constant K along the beam length, is the most resistant case against buckling. In the case of varying elastic foundation linearly, buckling load has the least amount comparing to the others. For all discussed elastic foundation variations, when porosity coefficients increase from 0 to 1, critical buckling load decreases by about 55 percent.

Effect of porosity coefficient on buckling load is shown in Fig. 4 for four boundary conditions. As can be seen, when porosity coefficient and aspect ratio enlarge, critical buckling loads decline. Also, it can be seen that the critical buckling load for Clamped-Clamped (CC) boundary conditions is higher than that of other boundary conditions.

To investigate the effect of porosity distribution on critical buckling load, three general types of distribution is considered including Eq. (19) for Type 1, Eq. (20) for Type 2 and Eq. (21) for Type 3. The other situations and parameters are the same as what was described earlier. It is

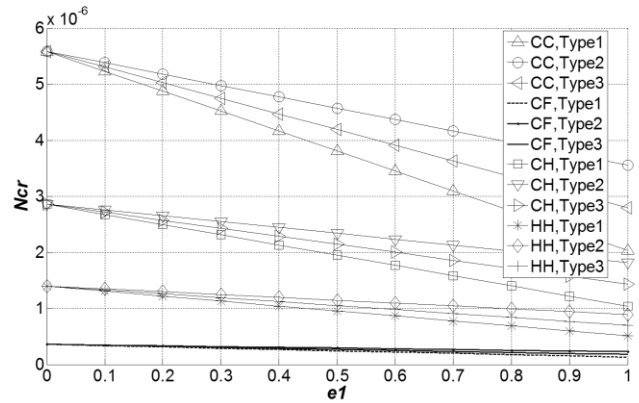


Fig. 4 Critical buckling load for three types of porosity distributions

Table 4 Comparing first three natural frequencies with the obtained results by Kacar *et al.* (2011)

K_f0	Natural Frequency	Kacar <i>et al.</i> (2011)	Present Work	Difference (%)
Constant	Ω_1	6.767	6.768	0.02
	Ω_2	7.724	7.538	-2.41
	Ω_3	9.972	8.753	-12.23
Linear	Ω_1	6.597	6.601	0.06
	Ω_2	7.614	7.418	-2.57
	Ω_3	9.922	8.677	-12.54
Parabolic	Ω_1	6.671	6.658	-0.19
	Ω_2	7.654	7.459	-2.55
	Ω_3	9.939	8.703	-12.44

obvious from Fig. 4, although the beginning point of three curves is the same, the differences rise by increasing porosity coefficient. It also can be seen that distribution Type 2 gives beam the most resistance against buckling. In contrast, beam with the distribution of porosity Type 1 is the least resistant one. Among four investigated boundary conditions, Clamped-Clamped (CC) and Clamped-Free (CF) create the most and the least buckling load.

5.2 Results and discussion of vibration

Results of vibration analysis of nano sandwich composite beam will be described in this section. Primarily, first three natural frequencies of a beam laying on variable elastic Winkler foundation defined in Eqs. (5-a) to (5-c) ($K0=2000$ and $\alpha=0.2$) are compared with the obtained results by Kacar *et al.* (2011) in Table 4. As can be seen, the results are in a good agreement. The results of first natural frequency as the most important one are pretty accurate.

Dimensionless natural frequency is defined in Eq. (23). Other parameters were described earlier.

$$\Omega = \sqrt[4]{\frac{\rho A \omega^2 L^4}{EI}} \quad (23)$$

First natural frequency against porosity coefficient in three different elastic foundations is presented in Fig. 5. It should be noted that clamped boundary conditions are

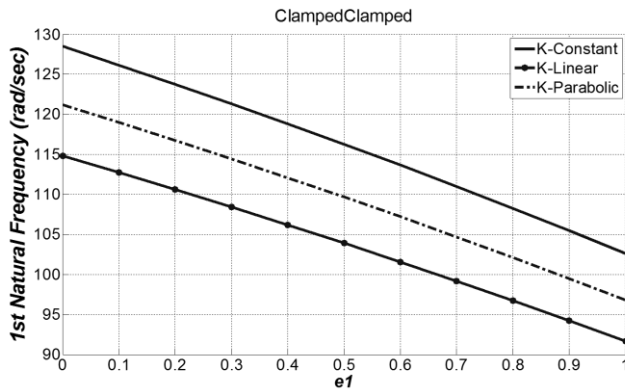


Fig. 5 First natural frequency against porosity coefficient for three kind of elastic foundations

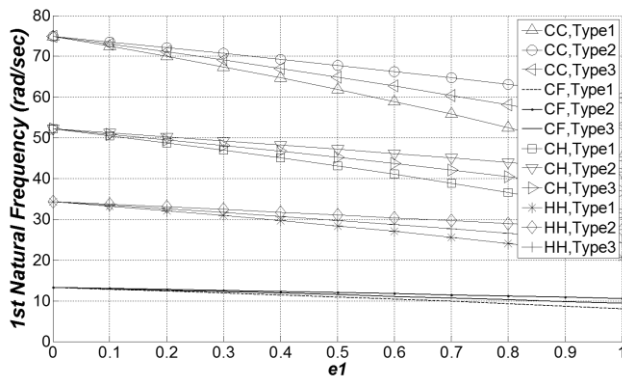


Fig. 6 First natural frequency for three types of porosity distributions

applied at two ends of the beam and K_f and α are assumed to be 1000 and 0.2, respectively. As could be seen, constant K along the beam length is the most suitable case to vibrational design. In the case of varying elastic foundation linearly, natural frequency has the least amount comparing to the others. While porosity coefficients increase from 0 to 1, first natural frequency decreases by about 20 percent. The mentioned result is almost the same for other elastic foundation variations. It should be noted the effect of the results achieved in the absence of shear spring will be discussed later.

To investigate the effect of porosity distribution on first natural frequency, three common types of distribution is considered including Eq. (19) for Type 1, Eq. (20) for Type 2 and Eq. (21) for Type 3. Elastic foundation assumed to be constants along beam length. The other situations and parameters are the same as what was described earlier. Fig. 6 shows the initial points of three curves are the same. The differences rise gradually by increasing porosity coefficient. It also can be seen that distribution Type 2 makes the beam resistant more against vibration. In contrast, beam with the distribution of porosity Type 1 has the least amount. Among four investigated boundary conditions, Clamped-Clamped (CC) and Clamped-Free (CF) have the most and the least natural frequency.

First natural frequency for three volume fractions (0.12, 0.17 and 0.28) of CNT and Clamped-Free boundary conditions for Configuration 1 is presented in Table 5.

Table 5 Natural frequency for three famous volume fractions of CNT and Clamped-Free boundary conditions for Configuration 1

		L/H	e_1	V_{cnt}	ω	V_{cnt}	ω	V_{cnt}	ω
Laminate 1	10		0		10298.280		10655.023		10917.895
			0.5		10328.675		10684.256		10942.328
			1		10359.344		10713.734		10966.927
	20		0	0.12	7303.476	0.17	7554.910	0.28	7737.394
			1		7325.163		7575.754		7754.788
			0		5945.715		6151.681		6303.450
30		0.5		5963.263		6168.558		6317.556	
		1		5980.970		6185.577		6331.758	
		0		225.590		233.436		222.687	
Laminate 2	10		0.5		186.828		193.285		184.291
			1		136.825		141.523		134.869
			0		159.516		165.064		157.463
	20		0.5	0.12	132.108	0.17	136.673	0.28	130.314
			1		96.750		100.072		95.367
			0		130.245		134.774		128.568
30		0.5		107.865		111.593		106.401	
		1		78.996		81.709		77.867	

Table 6 Natural frequency for three famous volume fractions of CNT and Clamped-Free boundary conditions for Configuration 2

		L/H	e_1	V_{cnt}	ω	V_{cnt}	ω	V_{cnt}	ω
Laminate 1	10		0		10430.913		11947.599		13759.679
			0.5		10461.705		11980.411		13790.559
			1		10492.776		12013.498		13821.651
	20		0	0.12	7397.543	0.17	8471.430	0.28	9751.398
			1		7419.513		8494.826		9773.383
			0		6022.290		6897.949		7944.154
30		0.5		6040.068		6916.893		7961.983	
		1		6058.007		6935.996		7979.934	
		0		205.616		247.916		247.209	
Laminate 2	10		0.5		170.279		205.267		204.580
			1		124.701		150.292		149.714
			0		145.393		175.303		174.803
	20		0.5	0.12	120.406	0.17	145.146	0.28	144.660
			1		88.177		106.272		105.864
			0		118.713		143.135		142.726
30		0.5		98.311		118.511		118.115	
		1		71.996		86.771		86.437	

Winkler and shear spring constants are considered to be 1000 and 200, respectively. Similar to buckling, it is concluded when aspect ratio of beam is more, natural frequency has smaller amount. Investigation of Laminates 1, 2 and 3 showed Laminate 2 has remarkably lower natural frequency than two other laminates which are absolutely close to each other. Porosity coefficients are considered to be 0, 0.5 and 1 in distribution Type 1. It is shown that when the porosity coefficient rises, the natural frequency increases slightly. It means in contrast to buckling, rigidity in natural frequency is more effective than density in the case of using shear spring.

Comparison between the results presented in Table 5, it

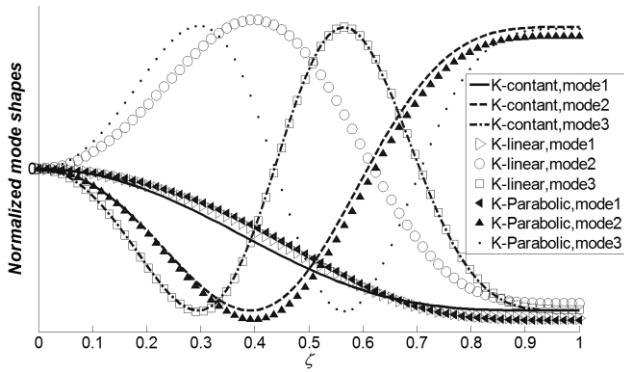


Fig. 7 First three vibration mode shapes for three kind of elastic foundations

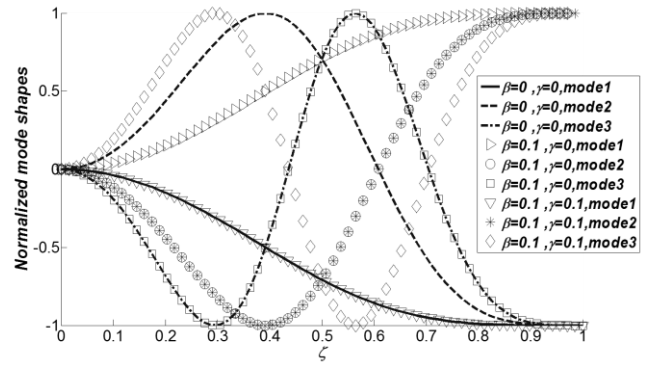


Fig. 8 The first three mode shapes of buckling of nano sandwich beam

is shown that natural frequency in Laminate 1 is much more than Laminate 2.

Similarity, Type 1 of porosity distribution is chosen and its coefficient is considered to be 0, 0.5 and 1. Comparing Table 5 and Table 6 demonstrates, when Configuration 2 is selected, first natural frequency increases about 26 percent in laminate 1 in the case of $V_{cm}=0.28$ and 12 percent in the case of $V_{cm}=0.17$. The amount of increase for laminate 2 is almost 12 and 6 percent by using $V_{cm}=0.28$ and 0.17 respectively.

In Figs. 7 and 8, the first three mode shapes of buckling of sandwich beam for three mentioned elastic foundations are presented. In all of them, Clamped-Free boundary condition is applied. Although the first mode shapes are the same for all of them, the second mode shapes are different when elastic foundation varies linearly along the length. It is also concluded that Third shape modes are unlike when variations of elastic foundations assumed parabolically.

5. Conclusions

In this article, the buckling and free vibration analysis of sandwich composite beam in two configurations of laminates using differential quadrature method (DQM) was investigated. The following results from this research can be listed as:

- It was concluded that for two configurations 1 and 2, Laminate 1 has remarkably larger buckling loads and natural frequencies than laminate 2.
- Comparing the two models, Model 2 (with thicker top and bottom part) has the more critical buckling load because of maximum bending which occurs at the outer layers. It also was shown that the influence of the core height on buckling load in the case of lower carbon volume fractions could be neglected. Even though, when volume fraction of fiber rises, differences increase gently. In addition, the effect is even more in the smaller beam aspect ratios.
- It was also shown in case of using Configuration 2, first natural frequency increases about 26 percent in laminate 1 in the case of $V_{cm}=0.28$ and 12 percent in the case of $V_{cm}=0.17$. The amount of increase (for mentioned carbon volume fraction) in laminate 2 is

almost 12 and 6 percent respectively.

- Investigating porosity coefficient presented that critical buckling load and natural frequency decreases linearly by increasing porosity coefficient in distribution Type 1. It should be noted the amount of decrease has inverse relationship with the aspect ratio of beam. On the other words, the effect of beam length is more than effect of porosity coefficient in buckling and vibration.

- It is known the maximum bending, which is leading to buckling, occurs in the top and bottom layers. So, the stiffer beam at the top and bottom, the more resistance against buckling. Results of this study showed that in case of porosity distribution Type 2, beam has the most resistance against buckling and vibration. Although with the mentioned distribution, beam is less strong at the top and bottom layers, because of choosing CNTRC as the material and making outer layers stiffer, the results are improved. It means the effect of porosity distribution in stiffness is less than material's selection in this case.

- Finally, among three discussed elastic foundation, buckling load and natural frequency in linear variation along length have the least amount comparing to the others. Because in linear case, the amount of lateral forces against buckling is the minimum compared to the others. For all of them, when porosity coefficients increase from 0 to 1, critical buckling load and first natural frequency decrease by about 55 and 20 percent respectively.

The most important advantage of the present work is designing a nanocomposite sandwich beam consists of a four-layer ($[45/90]_s$) FRC core and a three-layer ($[0/90/0]$) CNTRC at top and bottom by considering symmetric porosity distribution (the most porosity in the middle), on elastic foundation, which is more resistant against buckling and vibration.

Also, the differential quadrature method has the good convergence with lower node point numbers with respect to the other numerical method.

Acknowledgments

The authors would like to thank the reviewers for their valuable comments and suggestions to improve the clarity

of this work, and also they are thankful to the Iranian Nanotechnology Development Committee for their financial support and the University of Kashan for supporting this work by Grant No. 891238/18.

References

- Addou, F.Y., Meradjah, M., Bousahla, A.A., Benachour, A., Bourada, F., Tounsi, A. and Mahmoud, S.R. (2019), "Influences of porosity on dynamic response of FG plates resting on Winkler/Pasternak/Kerr foundation using quasi 3D HSDT", *Comput. Concrete*, **24**(4), 347-367. <https://doi.org/10.12989/cac.2019.24.4.347>.
- Al-Osta, M.A. (2019), "Shear behaviour of RC beams retrofitted using UHPFRC panels epoxied to the sides", *Comput. Concrete*, **24**(1), 37-49. <https://doi.org/10.12989/cac.2019.24.1.037>.
- Alimirzaei, S., Mohammadimehr, M. and Tounsi, A. (2019), "Nonlinear analysis of viscoelastic micro-composite beam with geometrical imperfection using FEM: MSGT electro-magneto-elastic bending, buckling and vibration solutions", *Struct. Eng. Mech.*, **71**(5), 485-502. <https://doi.org/10.12989/sem.2019.71.5.485>.
- Anirudh, B., Ganapathi, M., Anant, C. and Polit, O. (2019), "A comprehensive analysis of porous graphene-reinforced curved beams by finite element approach using higher-order structural theory: Bending, vibration and buckling", *Compos. Struct.*, **222**, 110899. <https://doi.org/10.1016/j.compstruct.2019.110899>.
- Anvari, M., Mohammadimehr, M. and Amiri, A. (2020), "Vibration behavior of a micro cylindrical sandwich panel reinforced by graphene platelet", *J. Vib. Control*, 1077546319892730. <https://doi.org/10.1177/1077546319892730>.
- Arefi, M., Kiani, M. and Rabczuk, T. (2019), "Application of nonlocal strain gradient theory to size dependent bending analysis of a sandwich porous nanoplate integrated with piezomagnetic face-sheets", *Compos. Part B: Eng.*, **168**, 320-333. <https://doi.org/10.1016/j.compositesb.2019.02.057>.
- Babaeian, M. and Mohammadimehr, M. (2020), "Investigation of the time elapsed effect on residual stress measurement in a composite plate by DIC method", *Opt. Laser Eng.*, **128**, 106002. <https://doi.org/10.1016/j.optlaseng.2020.106002>.
- Bahaadini, R. and Saidi, A.R. (2018), "Aeroelastic analysis of functionally graded rotating blades reinforced with graphene nanoplatelets in supersonic flow", *Aerosp. Sci. Technol.*, **80**, 381-391. <https://doi.org/10.1016/j.ast.2018.06.035>.
- Bamdad, M., Mohammadimehr, M. and Alambeigi, K. (2019), "Analysis of sandwich Timoshenko porous beam with temperature-dependent material properties: Magneto-electro-elastic vibration and buckling solution", *J. Vib. Control*, **25**(23-24), 2875-2893. <https://doi.org/10.1177/1077546319860314>.
- Barati, M.R. and Zenkour, A.M. (2018), "Analysis of postbuckling behavior of general higher-order functionally graded nanoplates with geometrical imperfection considering porosity distributions", *Mech. Adv. Mater. Struct.*, **26**(12), 1081-1088. <https://doi.org/10.1080/15376494.2018.1430280>.
- Batou, B., Nebab, M., Bennai, R., Atmane, H.A., Tounsi, A. and Bouremana, M. (2019), "Wave dispersion properties in imperfect sigmoid plates using various HSDTs", *Steel Compos. Struct.*, **33**(5), 699-716. <https://doi.org/10.12989/scs.2019.33.5.699>.
- Berghouti, H., Bedia, E.A.A., Benkhedda, A. and Tounsi, A. (2019), "Vibration analysis of nonlocal porous nanobeams made of functionally graded material", *Adv. Nano Res.*, **7**(5), 351-364. <https://doi.org/10.12989/anr.2019.7.5.351>.
- Boukhelif, Z., Bouremana, M., Bourada, F., Bousahla, A.A., Bourada, M., Tounsi, A. and Al-Osta, M.A. (2019), "A simple quasi-3D HSDT for the dynamics analysis of FG thick plate on elastic foundation", *Steel Compos. Struct.*, **31**(5), 503-516. <https://doi.org/10.12989/scs.2019.31.5.503>.
- Boulefrah, L., Hebali, H., Chikh, A., Bousahla, A.A., Tounsi, A. and Mahmoud, S.R. (2019), "The effect of parameters of visco-Pasternak foundation on the bending and vibration properties of a thick FG plate", *Geomech. Eng.*, **18**(2), 161-178. <https://doi.org/10.12989/gae.2019.18.2.161>.
- Bourada, F., Bousahla, A.A., Bourada, M., Azzaz, A., Zinata, A. and Tounsi, A. (2019), "Dynamic investigation of porous functionally graded beam using a sinusoidal shear deformation theory", *Wind Struct.*, **28**(1), 19-30. <https://doi.org/10.12989/was.2019.28.1.019>.
- Bui, T.Q., Nguyen, M.N. and Zhang, C. (2011), "An efficient meshfree method for vibration analysis of laminated composite plates", *Comput. Mech.*, **48**(2), 175-193. <https://doi.org/10.1007/s00466-011-0591-8>.
- Chaabane, L.A., Bourada, F., Sekkal, M., Zerouati, S., Zaoui, F.Z., Tounsi, A., Derras, A., Bousahla, A.A. and Tounsi, A. (2019), "Analytical study of bending and free vibration responses of functionally graded beams resting on elastic foundation", *Struct. Eng. Mech.*, **71**(2), 185-196. <https://doi.org/10.12989/sem.2019.71.2.185>.
- Chemi, A., Zidour, M., Heireche, H., Rakrak, K. and Bousahla, A.A. (2018), "Critical buckling load of chiral double-walled carbon nano tubes embedded in an elastic medium", *Mech. Compos. Mater.*, **53**(6), 827-836. <https://doi.org/10.1007/s11029-018-9708-x>.
- Chen, D., Yang, J. and Kitipornchai, S. (2015), "Elastic buckling and static bending of shear deformable functionally graded porous beam", *Compos. Struct.*, **133**, 54-61. <https://doi.org/10.1016/j.compstruct.2015.07.052>.
- Demirhan, P.A. and Taskin, V. (2019), "Bending and free vibration analysis of Levy-type porous functionally graded plate using state space approach", *Compos. Part B: Eng.*, **160**, 661-676. <https://doi.org/10.1016/j.compositesb.2018.12.020>.
- Draoui, A., Zidour, M., Tounsi, A. and Adim, B. (2019), "Static and dynamic behavior of nanotubes-reinforced sandwich plates using (FSDT)", *J. Nano Res.*, **57**, 117-135. <https://doi.org/10.4028/www.scientific.net/JNanoR.57.117>.
- Esawi, A.M. and Farag, M.M. (2007), "Carbon nanotube reinforced composites: Potential and current challenges", *Mater. Des.*, **28**(9), 2394-2401. <https://doi.org/10.1016/j.matdes.2006.09.022>.
- Fang, W., Yu, T., Lich, L.V. and Bui, T.Q. (2019), "Analysis of thick porous beams by a Quasi-3D theory and isogeometric analysis", *Compos. Struct.*, **221**, 110890. <https://doi.org/10.1016/j.compstruct.2019.04.062>.
- Ferreira, A.D.B., Novoa, P.R. and Marques, A.T. (2016), "Multifunctional material systems: A state-of-the-art review", *Compos. Struct.*, **151**, 3-35. <https://doi.org/10.1016/j.compstruct.2016.01.028>.
- Ghorbanpour Arani, A., Mobarakeh, M.R., Shams, S. and Mohammadimehr, M. (2012), "The effect of CNT volume fraction on the magneto-thermo-electro-mechanical behavior of smart nanocomposite cylinder", *J. Mech. Sci. Technol.*, **26**(8), 2565-2572. <https://doi.org/10.1007/s12206-012-0639-5>.
- Ghorbanpour Arani, A., Roustavi, B. and Mohammadimehr, M. (2016), "Surface stress and agglomeration effects on nonlocal biaxial buckling polymeric nanocomposite plate reinforced by CNT using various approaches", *Adv. Compos. Mater.*, **25**(5), 423-441. <https://doi.org/10.1080/09243046.2015.1052189>.
- Gui, X., Li, H., Zhang, L., Jia, Y., Liu, L., Li, Z., Wei, J., Wang, K., Zhu, H., Tang, Z., Wu, D. and Cao, A. (2011), "A facile route to isotropic conductive nanocomposites by direct polymer infiltration of carbon nano tube sponges", *ACS Nano*, **5**, 4276-4283. <https://doi.org/10.1021/nn201002d>.
- Hu, N., Fukunaga, H., Lu, C., Kameyama, M. and Yan, B. (2005),

- "Prediction of elastic properties of Carbon Nano Tube reinforced composites", *Proc. Royal Soc. A*, **461**, 1685-1710. <https://doi.org/10.1098/rspa.2004.1422>.
- Hussain, M. and Naeem, M.N. (2019), "Effects of ring supports on vibration of armchair and zigzag FGM rotating Carbon Nano Tubes using Galerkin's method", *Compos. Part B: Eng.*, **163**, 548-561. <https://doi.org/10.1016/j.compositesb.2018.12.144>.
- Jabbari, M. and Rezaei, M. (2016), "Mechanical buckling of FG saturated porous rectangular plate with piezoelectric actuators", *Iran. J. Mech. Eng.*, **17**(2), 45-65.
- Jabbari, M., Hashemitaheeri, M., Mojahedin, A. and Eslami, M.R. (2014), "Thermal buckling analysis of functionally graded thin circular plate made of saturated porous materials", *J. Therm. Stress.*, **37**(2), 202-220. <https://doi.org/10.1080/01495739.2013.839768>.
- Jabbari, M., Mojahedin, A., Khorshidvand, A.R. and Eslami, M.R. (2013), "Buckling analysis of a functionally graded thin circular plate made of saturated porous materials", *J. Eng. Mech.*, **140**(2), 287-295. [https://doi.org/10.1061/\(ASCE\)EM.1943-7889.0000663](https://doi.org/10.1061/(ASCE)EM.1943-7889.0000663).
- Kacar, A., Tan, H.T. and Kaya, M.O. (2011), "Free vibration analysis of beams on variable Winkler elastic foundation by using the differential transform method", *Math. Comput. Appl.*, **16**(3), 773-783. <https://doi.org/10.3390/mca16030773>.
- Karami, B., Janghorban, M. and Tounsi, A. (2019), "Wave propagation of functionally graded anisotropic nanoplates resting on Winkler-Pasternak foundation", *Struct. Eng. Mech.*, **7**(1), 55-66. <https://doi.org/10.12989/sem.2019.70.1.055>.
- Karami, B., Shahsavari, D., Janghorban, M. and Tounsi, A. (2019), "Resonance behavior of functionally graded polymer composite nanoplates reinforced with graphene nanoplatelets", *Int. J. Mech. Sci.*, **156**, 94-105. <https://doi.org/10.1016/j.ijmecsci.2019.03.036>.
- Kim, J., Zür, K.K. and Reddy, J.N. (2019), "Bending, free vibration, and buckling of modified couples stress-based functionally graded porous micro-plates", *Compos. Struct.*, **209**, 879-888. <https://doi.org/10.1016/j.compstruct.2018.11.023>.
- Kim, S.E., Duc, N.D., Nam, V.H. and Van Sy, N. (2019), "Nonlinear vibration and dynamic buckling of eccentrically oblique stiffened FGM plates resting on elastic foundations in thermal environment", *Thin Wall. Struct.*, **142**, 287-296. <https://doi.org/10.1016/j.tws.2019.05.013>.
- Kumar, P. and Srinivas, J. (2017), "Free vibration, bending and buckling of a FG-CNT reinforced composite beam: Comparative analysis with hybrid laminated composite beam", *Multidisc. Model. Mater. Struct.*, **13**(4), 590-611. <https://doi.org/10.1108/MMMS-05-2017-0032>.
- Liu, S., Yu, T., Yin, S. and Bui, T.Q. (2019), "Size and surface effects on mechanical behavior of thin nanoplates incorporating microstructures using isogeometric analysis", *Comput. Struct.*, **212**, 173-187. <https://doi.org/10.1016/j.compstruc.2018.10.009>.
- Magnucka-Blandzi, E. (2009), "Dynamic stability of a metal foam circular plate", *J. Theo. Appl. Mech.*, **47**(2), 421-433.
- Magnucka, E. (2008), "Axisymmetrical deflection and buckling of circular porous-cellular plate", *Thin Wall. Struct.*, **46**, 333-337. <https://doi.org/10.1016/j.tws.2007.06.006>.
- Magnucki, K. and Stasiewicz, P. (2004), "Elastic buckling of a porous beam", *J. Theo. Appl. Mech.*, **42**(4), 859-868.
- Magnucki, K., Malinowski, M. and Kasprzak, J. (2006), "Bending and buckling of a rectangular porous plate", *Steel Compos. Struct.*, **6**(4), 319-333. <https://doi.org/10.12989/scs.2006.6.4.319>.
- Mahmoudi, A., Benyoucef, S., Tounsi, A., Benachour, A., Adda Bedia, E.A. and Mahmoud, S.R. (2019), "A refined quasi-3D shear deformation theory for thermo-mechanical behavior of functionally graded sandwich plates on elastic foundations", *J. Sandw. Struct. Mater.*, **21**(6), 1906-1926. <https://doi.org/10.1177/1099636217727577>.
- Mao, J.J. and Zhang, W. (2019), "Buckling and post-buckling analyses of functionally graded graphene reinforced piezoelectric plate subjected to electric potential and axial forces", *Compos. Struct.*, **216**, 392-405. <https://doi.org/10.1016/j.compstruct.2019.02.095>.
- Medani, M., Benahmed, A., Zidour, M., Heireche, H., Tounsi, A., Bousahla, A.A., ... & Mahmoud, S.R. (2019), "Static and dynamic behavior of (FG-CNT) reinforced porous sandwich plate", *Steel Compos. Struct.*, **32**(5), 595-610. <https://doi.org/10.12989/scs.2019.32.5.595>.
- Mehar, K., Panda, S.K., Bui, T.Q. and Mahapatra, T.R. (2017), "Nonlinear thermoelastic frequency analysis of functionally graded CNT-reinforced single/doubly curved shallow shell panels by FEM", *J. Therm. Stress.*, **40**(7), 899-916. <https://doi.org/10.1080/01495739.2017.1318689>.
- Mohammadi, M., Saidi, A.R. and Jomehzadeh, E. (2010), "A novel analytical approach for the buckling analysis of moderately thick functionally graded rectangular plates with two opposite edges simply supported", *Mech. Eng. Sci.*, **224**, 1831-1841. <https://doi.org/10.1243/09544062JMES1804>.
- Mohammadimehr, M. and Alimirzaei, S. (2016), "Nonlinear static and vibration analysis of Euler-Bernoulli composite beam model reinforced by FG-SWCNT with initial geometrical imperfection using FEM", *Struct. Eng. Mech.*, **59**(3), 431-454. <http://dx.doi.org/10.12989/sem.2016.59.3.431>.
- Mohammadimehr, M. and Shahedi, S. (2017), "High-order buckling and free vibration analysis of two types sandwich beam including AL or PVC-foam flexible core and CNTs reinforced nanocomposite face sheets using GDQM", *Compos. Part B*, **108**, 91-107. <https://doi.org/10.1016/j.compositesb.2016.09.040>.
- Mohammadimehr, M., Hooyeh, H.M., Afshari, H. and Salarkia, M.R. (2017b), "Free vibration analysis of double-bonded isotropic piezoelectric Timoshenko micro-beam based on strain gradient and surface stress elasticity theories under initial stress stress using differential quadrature method", *Mech. Adv. Mater. Struct.*, **24**(4), 287-303. <https://doi.org/10.1080/15376494.2016.1142022>.
- Mohammadimehr, M., Okhravi, S.V. and Akhavan Alavi, S.M. (2018), "Free vibration analysis of magneto-electro-elastic cylindrical composite panel reinforced by various distributions of CNTs with considering open and closed circuits boundary conditions based on FSDT", *J. Vib. Control*, **24**(8), 1551-1569. <https://doi.org/10.1177/1077546316664022>.
- Mohammadimehr, M., Shahedi, S. and Roustavi, B. (2017a), "Nonlinear vibration analysis of FG-CNTRC sandwich Timoshenko beam based on modified couple stress theory subjected to longitudinal magnetic field using generalized differential quadrature method", *Proc. Inst. Mech. Eng., Part C: J. Mech. Eng. Sci.*, **231**(20), 3866-3885. <https://doi.org/10.1177/0954406216653622>.
- Montemurro, M., Vincenti, A. and Vannucci, P. (2012), "Design of the elastic properties of laminates with a minimum number of plies", *Mech. Compos. Mater.*, **48**(4), 369-390. <https://doi.org/10.1007/s11029-012-9284-4>.
- Ngo, T.D., Kashani, A., Imbalzano, G., Nguyen, K.T. and Hui, D. (2018), "Additive manufacturing (3D printing): A review of materials, methods, applications and challenges", *Compos. Part B: Eng.*, **143**, 172-196. <https://doi.org/10.1016/j.compositesb.2018.02.012>.
- Polit, O., Anant, C., Anirudh, B. and Ganapathi, M. (2019), "Functionally graded graphene reinforced porous nanocomposite curved beams: Bending and elastic stability using a higher-order model with thickness stretch effect", *Compos. Part B: Eng.*, **166**, 310-327. <https://doi.org/10.1016/j.compositesb.2018.11.074>.
- Radić, N. (2018), "On buckling of porous double-layered FG nanoplates in the Pasternak elastic foundation based on nonlocal

- strain gradient elasticity”, *Compos. Part B: Eng.*, **153**, 456-479. <https://doi.org/10.1016/j.compositesb.2018.09.014>.
- Rajabi, J. and Mohammadimehr, M. (2019a), “Hydro-thermo-mechanical biaxial buckling analysis of sandwich micro-plate with isotropic/orthotropic cores and piezoelectric/polymeric nanocomposite face sheets based on FSDT”, *Steel Compos. Struct.*, **33**(4), 509-523. <https://doi.org/10.12989/scs.2019.33.4.509>.
- Rajabi, J. and Mohammadimehr, M. (2019b), “Bending analysis of a micro sandwich skew plate using extended Kantorovich method based on Eshelby-Mori-Tanaka approach”, *Comput. Concrete*, **23**(5), 361-376. <https://doi.org/10.12989/cac.2019.23.5.361>.
- Semmah, A., Heireche, H., Bousahla, A.A. and Tounsi, A. (2019), “Thermal buckling analysis of SWBNNT on Winkler foundation by non local FSDT”, *Adv. Nano Res.*, **7**(2), 89-98. <https://doi.org/10.12989/anr.2019.7.2.089>.
- Shahedi, S. and Mohammadimehr, M. (2020), “Nonlinear high-order dynamic stability of AL-foam flexible cored sandwich beam with variable mechanical properties and carbon nanotubes-reinforced composite face sheets in thermal environment”, *J. Sandw. Struct. Mater.*, **22**(2), 248-302. <https://doi.org/10.1177/1099636217738908>.
- Shariat, B.A.S. and Eslami, M.R. (2007), “Buckling of thick functionally graded plates under mechanical and thermal loads”, *Compos. Struct.*, **78**(3), 433-439. <https://doi.org/10.1016/j.compstruct.2005.11.001>.
- Shen, M., Shi, Z., Zhao, C., Zhong, X., Liu, B. and Shu, X. (2019), “2-D meso-scale complex fracture modeling of concrete with embedded cohesive elements”, *Comput. Concrete*, **24**(3), 207-222. <https://doi.org/10.12989/cac.2019.24.3.207>.
- Sobhy, M. and Zenkour, A.M. (2019), “Porosity and inhomogeneity effects on the buckling and vibration of double-FGM nanoplates via a quasi-3D refined theory”, *Compos. Struct.*, **220**, 289-303. <https://doi.org/10.1016/j.compstruct.2019.03.096>.
- Sudheer, M., Pradyoth, K.R. and Somayaji, S. (2015), “Analytical and numerical validation of epoxy/glass structural composites for elastic models”, *Am. J. Mater. Sci.*, **5**(3C), 162-168. <https://doi.org/10.5923/c.materials.201502.32>.
- Syiemiong, H. and Marthong, C. (2019), “Effect of moisture on the compressive strength of low-strength hollow concrete blocks”, *Comput. Concrete*, **23**(4), 267-272. <https://doi.org/10.12989/cac.2019.23.4.267>.
- Tang, C.W. (2019), “Residual properties of high-strength fiber reinforced concrete after exposure to high temperatures”, *Comput. Concrete*, **24**(1), 63-71. <https://doi.org/10.12989/cac.2019.24.1.063>.
- Tang, H., Li, L. and Hu, Y. (2018), “Buckling analysis of two-directionally porous beam”, *Aerosp. Sci. Technol.*, **78**, 471-479. <https://doi.org/10.1016/j.ast.2018.04.045>.
- Thostenson, E.T., Ren, Z. and Chou, T.W. (2001), “Advances in the science and technology of carbon nano tubes and their composites: A review”, *Compos. Sci. Technol.*, **61**(13), 1899-1912. [https://doi.org/10.1016/S0266-3538\(01\)00094-X](https://doi.org/10.1016/S0266-3538(01)00094-X).
- Tornabene, F., Fantuzzi, N., Ubertini, F. and Viola, E. (2015), “Strong formulation finite element method based on differential quadrature: a survey”, *Appl. Mech. Rev.*, **02081**, 1-55. <https://doi.org/10.1115/1.4028859>.
- Wang, J., Chen, X., Bu, X. and Guo, S. (2019), “Experimental and numerical simulation study on fracture properties of self-compacting rubberized concrete slabs”, *Comput. Concrete*, **24**(4), 283-293. <https://doi.org/10.12989/cac.2019.24.4.283>.
- Wattanasakulpong, N. and Ungbhakorn, V. (2013), “Analytical solutions for bending, buckling and vibration responses of carbon nano tube-reinforced composite beams resting on elastic foundation”, *Comput. Mater. Sci.*, **71**, 201-208. <https://doi.org/10.1016/j.commatsci.2013.01.028>.
- Wu, H., Kitipornchai, S. and Yang, J. (2015), “Free vibration and buckling analysis of sandwich beams with functionally graded carbon nanotube-reinforced composite face sheets”, *Int. J. Struct. Stab. Dyn.*, **15**(7), 1540011-17. <https://doi.org/10.1142/S0219455415400118>.
- Wu, L. (2004), “Thermal buckling of a simply supported moderately thick rectangular FGM plate”, *Compos. Struct.*, **64**, 211-218. <https://doi.org/10.1016/j.compstruct.2003.08.004>.
- Xiang, S., Wang, J., Ai, Y.T. and Li, G.Ch. (2015), “Buckling analysis of laminated composite plates by using various higher-order shear deformation theories”, *Mech. Compos. Mater.*, **51**(5), 645-654. <https://doi.org/10.1007/s11029-015-9534-3>.
- Yas, M.H. and Samadi, N. (2012), “Free vibrations and buckling analysis of carbon nano tube-reinforced composite”, *Int. J. Press. Vess. Pip.*, **98**, 119-128. <https://doi.org/10.1016/j.ijpvp.2012.07.012>.
- Yazdani, R. and Mohammadimehr, M. (2019), “Double bonded Cooper-Naghdi micro sandwich cylindrical shells with porous core and CNTRC face sheets: Wave propagation solution”, *Comput. Concrete*, **24**(6), 499-511. <https://doi.org/10.12989/cac.2019.24.6.499>.
- Yazdani, R., Mohammadimehr, M. and Zenkour, A.M. (2019), “Vibration analysis of double-bonded micro sandwich cylindrical shells under multi-physical loadings”, *Steel Compos. Struct.*, **33**(1), 93-109. <https://doi.org/10.12989/scs.2019.33.1.093>.
- Yu, T., Hu, H., Zhang, J. and Bui, T.Q. (2019), “Isogeometric analysis of size-dependent effects for functionally graded microbeams by a non-classical quasi-3D theory”, *Thin Wall. Struct.*, **138**, 1-14. <https://doi.org/10.1016/j.tws.2018.12.006>.
- Yu, T., Zhang, J., Hu, H. and Bui, T.Q. (2019), “A novel size-dependent quasi-3D isogeometric beam model for two-directional FG microbeams analysis”, *Compos. Struct.*, **211**, 76-88. <https://doi.org/10.1016/j.compstruct.2018.12.014>.
- Zaoui, F.Z., Djamel Ouinas, D. and Tounsi, A. (2019), “New 2D and quasi-3D shear deformation theories for free vibration of functionally graded plates on elastic foundations”, *Compos. Part B: Eng.*, **159**, 231-247. <https://doi.org/10.1016/j.compositesb.2018.09.051>.
- Zghal, S., Frikha, A. and Dammak, F. (2017), “Static analysis of functionally graded carbon nano tube-reinforced plate and shell”, *Compos. Struct.*, **176**, 1107-1123.
- Zhang, H.S. (2010), “Thermal buckling and postbuckling behavior of functionally graded carbon nano tube-reinforced composite plates”, *Mater. Des.*, **31**(7), 3403-3411. <https://doi.org/10.1016/j.matdes.2010.01.048>.

CC